Existence and stability of rigid photovoltaic solitons in an open-circuit amplifying or absorbing photovoltaic medium

Jinsong Liu*

State Key Laboratory of Laser Technology, Huazhong University of Science and Technology, Wuhan 430074, China
(Received 12 December 2002; published 19 August 2003)

A different type of photovoltaic soliton is predicted for open-circuit photovoltaic media with a gain provided by two-wave mixing. Such solitons are a result of a double balance, i.e., loss is balanced by gain and diffraction is balanced by nonlinearity that is due to both, photovoltaic effects and two-wave mixing. Exact bright and dark analytical solutions are obtained under the condition that the signal beam is much weaker than the pump beam. Such solitons have fixed amplitude and width for the fixed values of the system parameters and hence are named *rigid photovoltaic solitons*. When the pump beam is switched to a background illumination, rigid photovoltaic solitons can become previously observed photovoltaic solitons. Numerical simulations show that rigid photovoltaic solitons are stable against small perturbations.

I. INTRODUCTION

Photovoltaic (PV) solitons in photovoltaic-photorefractive (PV-PR) crystals have been widely investigated theoretically [1–3] and experimentally [4–7]. In order to shorten the formation time of PV solitons, such as open-circuit PV bright solitons in a KNSBN crystal [4], people usually add uniform background irradiance to the entire crystal [4,5], in a manner similar to that to generate screening solitons [8]. Additional uniform background irradiance can be equivalent to effectively increasing the dark irradiance, which is typically very small (mW/cm^2) in all oxide and sillenite PV-PR materials, thus permitting observation of microwatt solitons with $0.1–1$ s response time in these materials [2]. Because the signal beam, i.e., the self-trapping beam and the background light usually come from a same laser, the background light is polarized strictly orthogonal to the polarization of the signal beam, such as the background light is an *o* ray when the signal beam is an *e* ray, which allows to avoid the possible coupling between the background and signal beams. In this paper, however, we predict that a different type of spatial solitons can exist if the polarizations of the two beams are not strictly orthogonal. In this case, the two beams can couple each other by PR two-wave mixing and hence the signal beam can obtain a gain from the background light that, in fact, has played a role as a pump beam. Such solitons have fixed amplitude and width for the fixed values of system parameters. Consequently, for the moment, we call them *rigid photovoltaic* (RPV) *solitons* that not only differ from the previously observed PV solitons in their properties and physical origins, but also have many important features. When the pump beam is switched to a background light, i.e., taking the polarization of the background light to be strictly orthogonal to the polarization of the signal beam, RPV solitons can become PV ones.

We already know that PV solitons come from PV effect [1–7] and quadratic solitons come from a three-wave mixing

process [9]. The RPV solitons are a result of the following two physical origins: PV effect and two-wave mixing. Unlike the investigations on quadratic solitons, in which the evolutions of both fundamental and second harmonic waves have been considered, the problem we are considering here is to investigate the evolution of the signal beam alone in a system consisting of an open-circuit PV-PR crystal and a pump beam with a uniform spatial distribution. Note that because the system can amplify or absorb the signal beam, hence it is a dissipative system in which soliton solutions are a result of a double balance, i.e., diffraction is balanced by nonlinearity and loss is balanced by gain. The double balance results in soliton solutions with fixed amplitude and width for the fixed values of system parameters because a total balance is possible only at some fixed values of system parameters [10]. Spatial solitons in some dissipative systems have been investigated, such as a weakly saturated amplifying or absorbing medium for an imaginary physical system theoretically [11] and a self-focusing semiconductor gain medium experimentally [12]. The propagation of a Gaussian light beam in a nonlinear medium with a complex susceptibility was discussed [13]. These investigations have shown that there is a significant difference between solitons in dissipative and Hamiltonian systems. We know that a system is a Hamiltonian one if it does not include the effects of both gain and loss, such as a PV-PR crystal when the effect of absorption is not taken into account. Soliton solutions in Hamiltonian systems are the result of a single balance between diffraction and nonlinearity. The single balance results in stationary solutions with arbitrary amplitude, which usually forms a one-parameter family [10]. PV solitons are supported by Hamiltonian systems, whereas RPV solitons are supported by dissipative ones. Therefore, RPV solitons must be significantly different from the previously observed PV solitons.

The concept of self-focusing or defocusing via wave mixing in biased PR crystals or PR oscillators and its application in soliton formation have been put forward by Vaupel and co-workers [14,15], in which the mechanism to support the self-focusing or defocusing arises from both, the spatially nonuniform screening of the applied field and two-wave mixing. Very recently, Cohen *et al.* [16] proposed a new kind

*Email address: jsliu4508@vip.sina.com
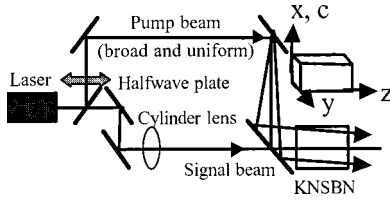
FIG. 1. The schematic of a rigid photovoltaic soliton in an open-circuit PV-PR crystal, in which the signal and pump beams are coupled to each other by PR two-wave mixing. C denotes the c axis of the crystal.

of spatial solitons, namely, holographic solitons that are solely supported by cross-phase modulation arising from the grating induced by PR two-wave mixing for the special case without energy exchange between the two beams. Hence the holographic solitons are supported by a Hamiltonian system.

In this paper, we develop a theory to describe the above open-circuit PV dissipative system in one dimension and steady state. We obtain a propagation equation of the signal beam and its exact bright and dark analytical solutions for the case that the signal beam is much weaker than the pump beam. Our results show that the signal beam can evolve into a bright (or dark) soliton. Numerical simulations show that these solitons are stable relative to small perturbations. We propose a relatively simple method to write down the propagation equation by simply treating the whole nonlinear process as a superposition of the PV effect and two-wave mixing. These two mechanisms, however, are the two aspects of the same phenomenon related to propagation and interaction of the two laser beams in PV-PR media. Hence the propagation equation should result from a general model such as the one introduced by Zozulya and Anderson [17]. By use of this model, some problems about the propagation of light beams in PR medium were investigated, such as snake instability and creation of optical vortices [18], symmetry breaking to spatial turbulence [19], as well as solitary attractors and low-order filamentation [20]. Nevertheless, our simple method allows us to avoid some cumbersome derivations and the result arising from the simple method will coincide with the final result arising from the general model for very weak index modulation and for soliton beam much weaker than the pump beam, however, which does not mean those two mechanisms act separately.

This paper is organized as follows. In Sec. II, the nonlinearity of the dissipative system is described and the propagation equation of the signal beam is derived. In Sec. III, the exact analytical bright and dark soliton solutions are obtained. In Sec. IV, the properties of the solitons are analyzed. In Sec. V, we do some numerical works to investigate the propagation and stability of the solitons as well as the influence of linear loss on the propagation and stability. Finally, we draw some conclusions in Sec. VI.

II. NONLINEAR AND WAVE EQUATION

Consider the schematic shown in Fig. 1. The crystal is taken here to be a doped KNSNB (such as Cu:KNSBN $Si_{0.25}Na_{0.75}Sr_{1.5}Br_5O_{15}$ [4]) with its optical c axis oriented

along the x coordinate. A one-dimensional signal beam is made to propagate along an ordinary principal axis (the z axis) and is itself extraordinarily polarized (along the x axis). The signal beam is confined in the x dimension, whereas it is extended (nondiffracting) in the second transverse direction, y. A strong pump beam with a uniform spatial distribution in both transverse dimensions also propagates along the z axis and makes a small angle θ with the signal beam in the crystal. The two coherent beams are coupled to each other by PR two-wave mixing and then the signal beam obtains a gain from the pump beam [21]. The pump beam is also a linearly polarized light and its polarized direction makes an angle φ with the x axis. Rotating the half-wave plate allows varying φ, and then allows controlling the value of γ_{eff}, the effective electro-optic coefficient of the two-wave mixing process [22]. The pump beam is an e ray (or an o ray) when $\varphi=0$ (or $\pi/2$). When $\varphi=\pi/2$, the pump beam, in fact, has become an ordinary polarized background illumination and $\gamma_{eff}=0$. In this case, this configuration has become the one that is needed for PV solitons [4–5], in which the ordinary polarization avoids the possible coupling between the background light and the self-trapping beam.

When the signal beam is much weaker than the pump beam, which makes a very weak index modulation, the perturbed extraordinary refractive index $\hat{n}_e$ for the signal beam can be written as $\hat{n}_e = n_e + \Delta n_1 + \Delta n_2$, where n_e is the unperturbed extraordinary refractive index and Δn_1 results from the PV effect and Δn_2 results from the two-wave mixing process. First, let us consider Δn_1, which can be expressed as [1] $\Delta n_1 = -n_e^3 r_{33} E_{sc}/2$, where r_{33} is the electro-optic coefficient, and E_{sc} is the space-charge field. Because the pump beam illuminates the entire crystal uniformly, it hence induces a uniform equivalent electric field [4]: $E_{eq} = -\kappa E_p$, where $\kappa = K_p^p/K_p^e$, and K_p^p and K_p^e are the PV coefficients of the pump and signal beams, respectively, and E_p is the PV field constant of the PV-PR crystal for the signal beam [1–4]. The equivalent electric field can be thought of as an externally applied field, as a result, when the dark irradiance is much weaker than the background beam, the space-charge field E_{sc} in the open-circuit PV-PR crystal can be expressed as [4] $E_{sc} = [I_b E_{eq} - I E_p]/(I + I_b)$, where $I = I(x,z)$ is the signal beam intensity and I_b is the background light intensity. For the system considered in this paper, we have $I_b = I_p$, where I_p is the pump beam intensity. Thereby we can obtain $E_{sc} = -E_p(\kappa I_p + I)/(I_p + I)$ and $\Delta n_1 = n_e^3 r_{33} E_p (I + \kappa I_p)/[2(I + I_p)]$. We then consider Δn_2, which can be found in Ref. [21] as $\Delta n_2 = n_1(e^{i\theta}\phi_p\phi^* e^{i\Delta} n_e/2\eta_0 + c.c.)/[2(I + I_p)]$, where ϕ and ϕ_p are the slowly varying envelopes of the electric-field component of the signal and pump beams, respectively, $I(x,z) = (n_e/2\eta_0)|\phi(x,z)|^2$, $I_p = (n_e/2\eta_0)|\phi_p|^2$, $\eta_0 = (\mu_0/\varepsilon_0)^{1/2}$, $\Delta = k_p z \cos\theta + k_p x \sin\theta - kz$, $k = n_e k_0$, $k_0 = 2\pi/\lambda_0$, λ_0 is the free-space wavelength of the lightwave employed and k and k_p are the wave vectors of the signal and pump beams, respectively. The term $n_1 e^{i\theta}$ can be expressed as $n_1 e^{i\theta} = \lambda_0(\Gamma_0 + i\Gamma/2)/\pi$, where Γ and Γ_0 are the intensity and phase coupling coefficients of the codirectional two-wave mixing process. Thus $\hat{n}_e$ can be expressed as

$$\hat{n}_e = n_e + \frac{n_e^3}{2} r_{33} E_p \frac{I + \kappa I_p}{I + I_p} + \left(\Gamma_0 + i\frac{\Gamma}{2}\right)\frac{n_e}{2\eta_0}\frac{\phi_p \phi^*}{I + I_p}\frac{e^{i\Delta}}{k_0} + \text{c.c.} \tag{1}$$

On the other hand, $n_1 e^{i\theta} = i n_e^3 \gamma_{\text{eff}} \tilde{E} E_s / (\tilde{E} + E_s)$, which results in $\Gamma_0 + i\Gamma/2 = i\delta\tilde{E}E_s/(\tilde{E}+E_s)$, where $\delta = n_e^3 \gamma_{\text{eff}} k_0/2$, $\tilde{E} = E_d - iE_{\text{eq}}$, $E_d = 4\pi k_B T \sin\theta/(\lambda_0 e)$ is the diffusion field, k_B is the Boltzmann constant, e is the electron charge, T is the absolute temperature, $E_s = eN_A\lambda_0/(4\pi\varepsilon\varepsilon_0 \sin\theta)$ is the saturation field, N_A is the acceptor density, ε is the effective dielectric constant, and ε_0 is the permittivity of vacuum. The expression for γ_{eff} is $\gamma_{\text{eff}} = \tilde{\gamma}_{\text{eff}}(\hat{e}\cdot\hat{e}_p)$, where $\hat{e}$ and $\hat{e}_p$ are the polarization vectors of the signal and pump beams, respectively [22]. For the configuration described above, $\tilde{\gamma}_{\text{eff}} = \bar{n}^3\gamma_{33}\cos\theta\cos(\theta/2) + \bar{n}\gamma_{42}\sin(\theta)\sin(\theta/2)$ and $(\hat{e}\cdot\hat{e}_p) = \cos\varphi$, where $\bar{n} = n_e/n_0$, n_0 is the ordinary refractive index. Thus we have

$$\gamma_{\text{eff}} = \bar{n}[\bar{n}^2\gamma_{33}\cos\theta\cos(\theta/2) + \gamma_{42}\sin(\theta)\sin(\theta/2)]\cos\varphi. \tag{2}$$

Note that, when the pump beam is taken as an ordinary polarized background illumination, we have $\varphi = \pi/2$, which results in $\gamma_{\text{eff}} = 0$ and hence $\Gamma = \Gamma_0 = 0$.

By use of a way similar to that in Ref. [21], in which the coupled-wave equation for two-wave mixing was derived, but then considering the variation of ϕ in the x direction, using Eq. (1) as the expression for the perturbed refractive index and ignoring the quadratic terms of Δn_1 and Δn_2 as well as the products of Δn_1 and Δn_2, in the slowly varying approximation (i.e., ignoring the term of $\partial^2\phi/\partial z^2$), we find that ϕ satisfies the following paraxial wave equation:

$$\frac{1}{2k}\frac{\partial^2\phi}{\partial x^2} + i\frac{\partial\phi}{\partial z} + k_0\frac{n_e^3}{2}\gamma_{33}E_P\frac{I+\kappa I_p}{I+I_p}\phi + \left(\Gamma_0 - \frac{i}{2}\Gamma\right)\frac{I_p}{I+I_p}\phi$$

$$+ i\frac{1}{2}\alpha_0\phi = 0, \tag{3}$$

where α_0 is the absorption coefficient of the crystal. We now rewrite the wave equation in a dimensionless form by letting $s = x/x_0$, $\xi = z/z_0$, $z_0 = kx_0^2$, and $U = (2\eta_0 I_p/n_e)^{-1/2}\phi$, where x_0 is an arbitrary spatial width. Thus we get a dynamical evolution equation in term of U as the following:

$$i\frac{\partial U}{\partial\xi} + \frac{1}{2}\frac{\partial^2 U}{\partial s^2} + \sigma\frac{|U|^2+\kappa}{1+|U|^2}U + (g_0 - ig)\frac{U}{1+|U|^2} + i\alpha U$$

$$= 0, \tag{4}$$

where $\sigma = \chi\gamma_{33}E_p$, $\chi = (k_0 x_0)^2 n_e^4/2$, $g_0 = z_0\Gamma_0$, $g = z_0\Gamma/2$, and $\alpha = z_0\alpha_0/2$. From $\Gamma_0 + i\Gamma/2 = i\delta\tilde{E}E_s/(\tilde{E}+E_s)$, we can obtain the expressions for g and g_0 as $g = \chi\gamma_{\text{eff}}E_s(E_{\text{eq}}^2 + E_d E_{ds})/(E_{ds}^2 + E_{\text{eq}}^2)$ and $g_0 = \chi\gamma_{\text{eff}}E_{\text{eq}}E_s^2/(E_{ds}^2 + E_{\text{eq}}^2)$, where $E_{ds} = E_d + E_s$.

III. EXACT ANALYTICAL SOLUTIONS

It is difficult to obtain an exact analytical solution of Eq. (4) in general conditions. In what follows, we solve this equation in the condition of $|U|^2 = I/I_p \ll 1$, thereby we can take $(1+|U|^2)^{-1} \approx 1 - |U|^2$, and thus the last equation becomes

$$i\frac{\partial U}{\partial\xi} + \frac{1}{2}\frac{\partial^2 U}{\partial s^2} + (Q - iG)U + (P + ig)U|U|^2 = 0, \tag{5}$$

where $Q = \kappa\sigma + g_0$, $G = g - \alpha$, and $P = \sigma(1-\kappa) - g_0$.

In order to find the exact analytical solutions of Eq. (5), we should assume the pump beam intensity I_p to be constant for each value of z. If the crystal has a small absorption coefficient and the intensity coupling between the signal and pump beams is quite weak, the approximation could be satisfied very well. Selecting a value of φ, which is close to $\pi/2$, can allow the condition of weak intensity coupling to be satisfied. For a constant value of I_p, we can use the results in Refs. [10], [23] to obtain the exact analytical bright and dark soliton solutions of Eq. (5). To do so, let

$$U(s,\xi) = P^{-1/2}V(s,\xi)e^{iQ\xi}; \tag{6}$$

Eq. (5) then becomes a standard cubic complex Ginzburg-Landau equation, but without the term of spatial spectral filtering, as the following:

$$i\frac{\partial V}{\partial\xi} + \frac{1}{2}\frac{\partial^2 V}{\partial s^2} + V|V|^2 = iGV - i\frac{g}{P}V|V|^2. \tag{7}$$

The bright soliton solutions of Eq. (7) can be directly written as $V(s,\xi) = FP^{1/2}\sec h(Bs)\exp\{ib\ln[\sec h(Bs)]\}\exp[-i(\nu + Q)\xi]$ [10]. Inserting it into Eq. (6), we obtain the bright soliton solution of Eq. (5) as the following:

$$U(s,\xi) = F\sec h(Bs)\exp\{ib\ln[\sec h(Bs)]\}\exp(-i\nu\xi), \tag{8}$$

where $F = [3G/(2g)]^{1/2}$, $B = (G/b)^{1/2}$, $b = [-3P+(9P^2 + 8g^2)^{1/2}]/(2g)$, and $\nu = (b^2-1)G/(2b) - Q$. Dark soliton solutions of Eq. (7) have been found in Ref. [23] and refined in Ref. [24] and can be written as $V(s,\xi) = DP^{1/2}\tanh(Hs)\exp\{id\ln[\cosh(Hs)]\}\exp[-i(\Omega+Q)\xi]$. Inserting it into Eq. (6), we obtain the dark soliton solution of Eq. (5) as the following:

$$U(s,\xi) = D\tanh(Hs)\exp\{id\ln[\cosh(Hs)]\}\exp(-i\Omega\xi), \tag{9}$$

where $D = (G/g)^{1/2}$, $H = [2G/(3d)]^{1/2}$, $d = [3P+(9P^2 + 8g^2)^{1/2}]/(2g)$, and $\Omega = 2G/(3d) - Q$. In solutions (8) and (9), F and D are the amplitudes, B and H are the parameters associated with the width, ν and Ω represent the nonlinear shifts of the propagation constant, b and d are the chirp parameters. These solutions show that bright and dark spatial solitons, so-called RPV solitons, can exist in an open-circuit PV-PR crystal with a gain of two-wave mixing.

If the pump beam is switched to a background illumination, the absorption of the crystal is neglected and the

equivalent electric field induced by the pump beam is not taken into account, we have $g=g_0=0$, $\kappa=0$, and $\alpha\to 0$, thus $P=\sigma$ and $Q=0$. For the bright soliton case, we have, $F\to r^{1/2}$, $B\to(r\sigma)^{1/2}$, $\nu\to 0$, and $b\to 2g/(3P)\to\mathbf{0}$, where r $[=\lim_{g,\alpha\to 0} 3(g-\alpha)/(2g)]$ is an arbitrary positive parameter, i.e., the amplitude of the soliton as a free parameter. In this case, Eq. (8) reduces into the solution of weak amplitude PV bright solitons as the following:

$$U(s,\xi)=\sqrt{r}\sec h(\sqrt{r\sigma}s). \qquad (10)$$

An expression equivalent to this solution can be found in Ref. [2]. The necessary condition for the soliton is $\sigma>0$, i.e., $E_p>0$. For the dark soliton case, we have $D\to\rho^{1/2}$, $H\to[-\rho\sigma)]^{1/2}$, $\Omega\to 0$, and $d\to-2g/(3P)\to 0$, where ρ $[=\lim_{g,\alpha\to 0}(g-\alpha)/g]$ is an arbitrary positive parameter. Solution (9) reduces into the solution of weak amplitude PV dark solitons as the following:

$$U(s,\xi)=\sqrt{\rho}\tanh(\sqrt{-\rho\sigma}s). \qquad (11)$$

An expression equivalent to this solution can be found in Ref. [2]. The necessary condition for this dark soliton is $\sigma<0$, i.e., $E_p<0$. The above results indicate that the system of a PV-PR crystal with a two-wave mixing gain can be easily switched from a dissipative system to a Hamiltonian one by switching the pump beam to a background illumination, and vice versa. As a result, the RPV solitons can then be easily switched from the "rigid" ones, i.e., with fixed amplitude and width, to the "soft" ones, i.e., with arbitrary amplitude. The idea of switching a soliton from rigid state to soft one was presented first by Akhmediev and co-workers, and the system considered here is a physical counterpart for their theoretical one [10]. This knowledge is important for designing new types of an all-optical switch.

IV. PROPERTIES OF RPV SOLITONS

In order to analyze the properties of RPV solitons, it is necessary to make some detailed calculations. In doing so, in this section and the following sections, we take $n_e=2.27$, $n_0=2.35$, $\varepsilon=500$, $\gamma_{42}=820$ pm/V, and $\gamma_{33}=200$ pm/V for a KNSBN crystal at $\lambda_0=0.5$ μm. The value of κ and E_p depends on the polarization of the pump beam and the intensity of the signal beam. The experimental results in Ref. [4] show that when the pump beam is an o ray and the signal beam is an e ray, the ratio $\kappa=K_p^p/K_p^e=K_p^o/K_p^e=0.4$ and when the beam intensity in the crystal is about 8 W/cm^2 (at $\lambda_0=0.488$ μm), the PV field constant $E_p=27$ KV/cm. On the other hand, we have $\kappa=K_p^p/K_p^e=K_p^e/K_p^e=1$ if the pump beam is also an e ray. Consequently, if the pump beam has both ordinary and extraordinary polarization components, the value of κ will be in the range of (0.4, 1), so we can approximately take $\kappa=0.5$ for $\varphi=87°$ and, if the signal beam intensity is taken as $I=800$ mW/cm^2, we can approximately take $E_p=3000$ V/cm. The other parameters are taken as $N_A=1.2\times 10^{16}$ cm^{-3}, $x_0=15$ μm, $\theta=2°$, and $T=300$ K.

At first, let us consider the conditions necessary for RPV solitons, which are $g>\alpha$ and $b>0$ (or $d>0$) for bright (or
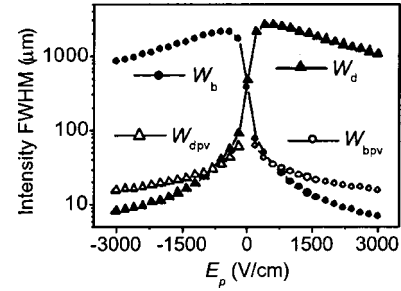
FIG. 2. The intensity FWHM varying with the PV field constant at $\alpha=0.09$. $r=0.1$ and $\rho=0.1$ for bright and dark PV solitons, respectively.

dark) case. From the definitions of b, d, and P we know that b and d are always positive whether $P>0$ or <0. That is, both bright and dark RPV solitons can exist whether $P>0$ or <0, which results in the fact that both bright and dark RPV solitons can exist whether $E_p>0$ or <0. This result presents a striking contrast to the fact that the bright (or dark) PV soliton can exist only if $E_p>0$ (or <0) [1–3]. Notice that $P>0$ or <0 means that the crystal possesses a focusing or defocusing nonlinearity. Therefore, both bright and dark RPV solitons can exist whether the medium possesses a focusing or defocusing nonlinearity, just as do the spatial solitons in other dissipative systems [11–13], whereas bright or dark PV solitons can exist when the medium possesses only a focusing or defocusing nonlinearity [1–3].

We then consider the soliton width [intensity FWHM (full width at half maximum)]. Although either focusing or defocusing nonlinearity can support a bright (or dark) RPV soliton, the soliton width depends strongly on the feature of the nonlinearity. Let W_b and W_d denote the intensity FWHM of bright and dark RPV solitons, respectively, from Eqs. (8) and (9), then we have $W_b=1.76x_0/B$ and $W_d=1.76x_0/H$. In order to compare them with that of weak amplitude PV solitons, from Eqs. (10) and (11), we have $W_{bpv}=1.76x_0(r\sigma)^{-1/2}$ and $W_{dpv}=1.76x_0(-\rho\sigma)^{-1/2}$, which denote the intensity FWHM of weak amplitude bright and dark PV solitons, respectively. Whether the crystals possess a focusing or defocusing nonlinearity depends on the sign of E_p. If a positive E_p makes a focusing nonlinear, a negative one must also make a defocusing nonlinear [26]. Some PV crystals possess a PV field constant with a deterministic sign, such as $E_p<0$ for LiNbO$_3$ [2,25], whereas some PV crystals (for example, BaTiO$_3$) possess PV field constants that change sign under polarization rotation [25]. Although the sign of E_p for a given crystal and beam polarization is given, in order to provide a panoramic view, we calculate the E_p dependence of the width of RPV solitons for E_p varying from negative to positive values as shown in Fig. 2. When $E_p>0$ (or $E_p<0$), W_b (or W_d) decreases as E_p (or $|E_p|$) increases, whereas when $E_p<0$ (or $E_p>0$), W_b (or W_d) increases and, reaches its maximum value at a character E_p and then decreases as $|E_p|$ (or E_p) increases. Both W_b and W_d are very sensitive to E_p when E_p is near the zero point. W_{bpv} (or W_{dpv}) has a behavior similar to that for W_b (or W_d) when $E_p>0$ (or $E_p<0$). The crystal possesses a focusing or defocusing nonlinearity when $E_p>0$ or $E_p<0$ because P is
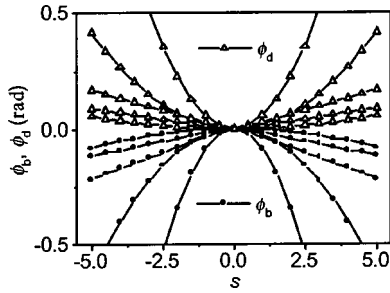
FIG. 3. Phase profiles of a bright and dark RPV soliton, ϕ_b and ϕ_d, at $\alpha = 0.09$. The circles denote ϕ_b for $E_p = 0$, 1500, 3000, -1500, -3000 (from top to bottom). The triangles denote ϕ_d for $E_p = 3000$, 1500, -3000, -1500, 0 (from top to bottom).

FIG. 4. Simultaneous propagation of a RPV bright soliton (intensity profiles). System parameters: $\alpha = 0.17$, $g = 0.26$, $g_0 = -0.56$, $\sigma = 28$, and $\kappa = 0.4$. Solution parameters: $F = 0.72$, $B = 2.7$, $b = 0.012$, and $\nu = -17$. Input conditions: $\Delta F = 0$ and $\Delta B = 0$.

positive when $E_p > 0$, whereas negative when $E_p < 0$. The above results show that although either focusing or defocusing nonlinearity can support a RPV bright (or dark) soliton, the width of the soliton is much narrower in the focusing (or defocusing) case than that in the defocusing (or focusing) case.

Finally, we consider the wave front of RPV solitons. Letting $\phi_b(s)$ and $\phi_d(s)$ denote the wave fronts of bright and dark RPV solitons, respectively, from solutions (8) and (9), we have

$$\phi_b = b\ln[\sec h(Bs)] \approx \begin{cases} -[(g-\alpha)/2]s^2, & s \leq W_b/3.53 \\ b(\ln 2 \pm Bs), & s > W_b/3.53, \end{cases} \tag{12}$$

$$\phi_d = d\ln[\cosh(Hs)] \approx \begin{cases} [(g-\alpha)/3]s^2, & s \leq W_d/3.53 \\ -d(\ln 2 \pm Hs), & s > W_d/3.53. \end{cases} \tag{13}$$

Obviously, RPV solitons have nonuniform wave front, which are parabolic near axis and become progressively linear off-axis, whereas PV solitons have uniform wave front [1–3]. As mentioned above, the focusing (or defocusing) nonlinearity creates smaller values of W_b (or W_d), whereas the defocusing (or focusing) nonlinearity creates larger values of W_b (or W_d). As a result, the linear function will dominate ϕ_b (or ϕ_d) for focusing (or defocusing) case, whereas the parabolic function will dominate ϕ_b (or ϕ_d) for defocusing (or focusing) case. Because b, d, B, and H depend on E_p, the wave front profiles will change with E_p (see Fig. 3). As we can see, $\phi_b < 0$ and $\phi_d > 0$. Thereby, bright and dark RPV solitons are divergent and converging beams, respectively.

V. PROPAGATION AND STABILITY OF RPV SOLITONS

In this section, we investigate the questions of the propagation and stability of bright RPV solitons by use of a numerical approach. The values of n_e, n_0, ε, γ_{42}, γ_{33}, N_A, κ, E_p, φ, θ, λ_0, x_0, and T are taken as same as given in Sec. IV. From these values, we have $\Gamma = 0.81$ cm^{-1} and $\Gamma_0 = -0.88$ cm^{-1}. First, let us consider the propagation of a bright RPV soliton at $\alpha_0 = 0.54$ cm^{-1}. The corresponding values of those dimensionless system parameters in Eq. (5) are $\alpha = 0.17$, $g = 0.26$, $g_0 = -0.56$, $\sigma = 28$, and $\kappa = 0.5$. Tak-

ing these values into Eq. (8), we get a bright RPV soliton with the following values of the solution parameters $F = F_0 = 0.71$, $B = B_0 = 2.7$, $b = b_0 = 0.012$, and $\nu = \nu_0 = -17$. This bright RPV soliton possesses a width (intensity FWHM) to be 9.7 μm and a ratio of $I/I_p = F_0^2 = 0.49$. The dynamical evolution of the solitary beam can be obtained by numerically solving Eq. (5) with the above values of α, g, g_0, σ, and κ. As expected, our results confirm that the soliton states remain invariant with propagation distance, as shown in Fig. 4 (calculated to $\xi = 10$, i.e., $z \approx 6.7$ cm).
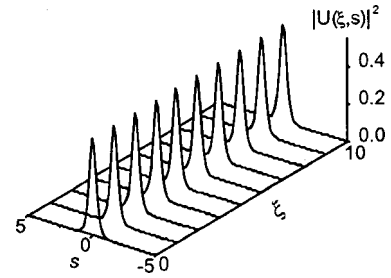
We then consider the stability of these solitons relative to small perturbations of the initial conditions. In general, a soliton is stable if, after a small perturbation, it approaches some stationary state. We have studied the stability of the solitons numerically, by adding small perturbations to exact solution (8) and solving the full nonlinear equation (5). To do so, by taking $F = F_0 + \Delta F$, $B = B_0 + \Delta B$, $b = b_0$, and $\nu = \nu_0$ into Eq. (8), we can get a beam whose amplitude and width are slightly different from those of an exact solution of Eq. (5). The dynamical evolution of these pretreated beams can then be obtained by numerically solving Eq. (5) with the above values of the dimensionless system parameters. Figure 5 shows an example for $z = 3.4$ cm. As we can see, the beam reshapes itself and tries to evolve into a solitary wave in the medium. Our calculations also show that for this set of system parameters, when $|\Delta F| \leq 0.04$ and $\Delta B = 0$ as well as $\Delta F = 0$ and $|\Delta B| \leq 0.1$, these solitons are stable. Figures 6 and 7 give the dynamics of the peak solitary beam intensity for different values of ΔF and ΔB. When $\Delta F \neq 0$ or $\Delta B \neq 0$, the intensity converges toward $\Delta F = 0$ and $\Delta B = 0$.
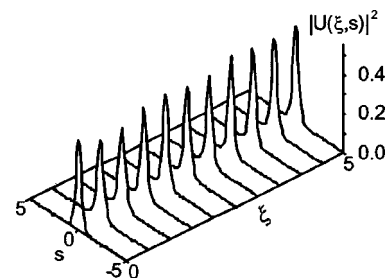
FIG. 5. Dynamical evolution towards the solitary wave (intensity profiles). System and solution parameters are the same as in Fig. 4. Input conditions: $\Delta F = -0.04$ and $\Delta B = 0$.
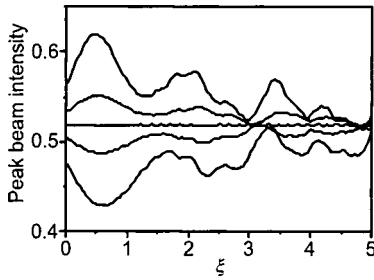
FIG. 6. Dynamics of the normalized peak solitary beam intensity. System and solution parameters are the same as in Fig. 4. Input conditions: $\Delta B = 0$ and $\Delta F = 0.04, 0.01, 0, -0.01, -0.04$ (from top to bottom).

These results indicate that the bright RPV solitons are stable against small perturbations in both amplitude and width.

Finally, we consider the influence of linear loss on the propagation of RPV solitons in PV-PR crystals. In Eq. (5), $G = g - \alpha$ denotes a net gain. Different values of G will appear for different values of α. The beam at the input is assumed to be a bright soliton solution of Eq. (5), i.e., solution (8) with $F = 0.72$, $B = 2.7$, $b = 0.012$, and $\nu = -17$, coming from the system parameters $\alpha = 0.17$, $g = 0.26$, $g_0 = -0.56$, $\sigma = 28$, and $\kappa = 0.5$ with a net gain $G = G_0 = 0.09$. Let $\Delta G = G - G_0$ denote the variation in the net gain when $\alpha \neq 0.17$. The evolution of the beam in the crystal is then investigated by solving Eq. (5) with $g = 0.26$, $g_0 = -0.56$, $\sigma = 28$, and $\kappa = 0.4$ for $\alpha = 0, 0.13, 0.17, 0.2$, and 0.25 (the corresponding actual values are $\alpha_0 = 0, 0.41, 0.54, 0.62$, and 0.78 cm^{-1}), which makes $\Delta G = 0.17, 0.04, 0, -0.03$, and -0.07, respectively. The dynamics of the beam in the crystal is depicted in Fig. 8. The figures show that the beam exhibits a different evolution feature for different sign of ΔG. When $\Delta G < 0$, which corresponds to the excess loss case, the intensity of the beam decreases with propagation distance because the gain cannot overcome the loss and then the beam is progressively absorbed as it propagates and, consequently, the beam cannot evolve into a stable RPV soliton irrespective of how large $|\Delta G|$ is, as shown in Figs. 8(a) and 8(b). However, when $\Delta G > 0$, which corresponds to the excess gain case, the intensity of the beam incessantly increases with propagation distance and the beam finally becomes a divergent one for a big value of ΔG, such as $\Delta G = 0.17$, as shown in Fig. 8(c),
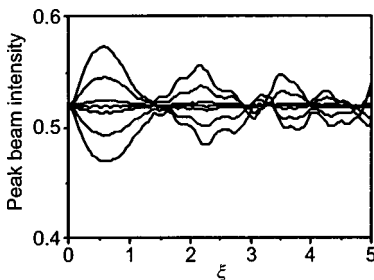
FIG. 7. Dynamics of the normalized peak solitary beam intensity. System and solution parameters are the same as in Fig. 4. Input conditions: $\Delta F = 0$ and $\Delta B = -0.1, -0.05, -0.01, 0, 0.01, 0.05, 0.1$ (from top to bottom).
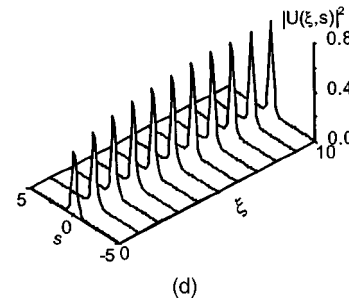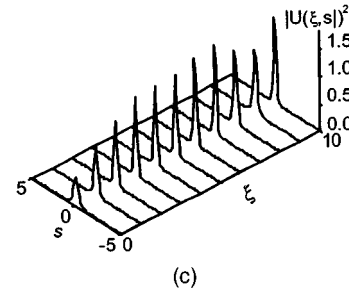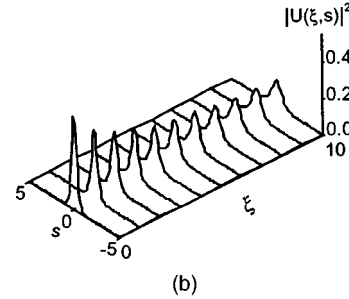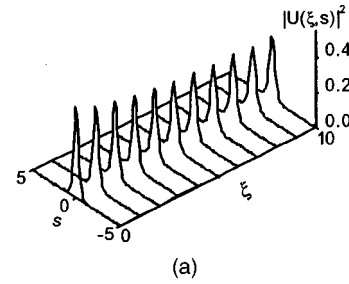
FIG. 8. The effect of loss on the evolution of a beam in a PV amplifying or absorbing system. The input beam is a bright RPV solitary solution with $F = 0.72$, $B = 2.7$, $b = 0.012$, and $\nu = -17$. The system parameters are $g = 0.26$, $\sigma = 28$, $\beta = -14$, $g_0 = -0.56$; and (a) $\alpha = 0.2$, $\Delta G = -0.03$; (b) $\alpha = 0.25$, $\Delta G = -0.07$; (c) $\alpha = 0$, $\Delta G = 0.17$, and (d) $\alpha = 0.13$, $\Delta G = 0.04$.

whereas the intensity of the beam is amplified initially and then reaches a saturation value, and the beam finally evolves into a stable RPV soliton for a small value of ΔG, such as $\Delta G = 0.04$, as shown in Fig. 8(d). In the last case, the beam loses its energy until it converges to a stationary state and the self-trapping is then said to be stable.

VI. CONCLUSION

We suggest using a KNSBN crystal with a configuration, which can be obtained by putting a half-wave plate into the

illuminate beam path in the configuration needed for PV solitons [4], to generate and observe RPV solitons. In order to observe the soliton beam without disturbing from the pump beam, one can take a manner, which is similar to that for monitoring the incoherently coupled PR soliton pairs [27,28], to monitor RPV solitons.

In conclusion, we have shown that a different type of soliton can exist in open-circuit PV-PR materials when the self-trapping beam couples coherently with a pump beam by two-wave mixing, obtained an exact analytical solution for the soliton under the condition that the pump beam is much stronger than the self-trapping beam, discussed the unique properties and stability of these solitons as well as the influence of linear loss on the propagation and stability, and considered the configuration and methods necessary for generating and observing RPV solitons.

[1] G. C. Valley, M. Segev, B. Crosignani, A. Yariv, M. M. Fejer, and M. C. Bashaw, Phys. Rev. A **50**, R4457 (1994).

[2] M. Segev, G. C. Valley, M. C. Bashaw, M. Taya, and M. M. Fejer, J. Opt. Soc. Am. B **14**, 1772 (1997).

[3] J. Liu and K. Lu, J. Opt. Soc. Am. B **16**, 550 (1999).

[4] W. L. She, K. K. Lee, and W. K. Lee, Phys. Rev. Lett. **83**, 3182 (1999).

[5] M. Taya, M. C. Bashaw, M. M. Fejer, M. Segev, and G. C. Vally, Phys. Rev. A **52**, 3095 (1995).

[6] M. Taya, M. C. Bashaw, M. M. Fejer, M. Segev, and G. C. Valley, Opt. Lett. **21**, 943 (1996).

[7] Z. Chen, M. Segev, D. W. Wilson, R. E. Muller, and P. D. Maker, Phys. Rev. Lett. **78**, 2948 (1997).

[8] K. Kos, H. X. Meng, G. Salamo, M. Shih, M. Segev, and G. C. Valley, Phys. Rev. E **53**, R4330 (1996).

[9] W. Torruellas, Y. S. Kivshar, and G. I. Stegeman, in *Spatial Solitons*, edited by S. Trillo and W. Torruellas (Springer, Berlin, 2001), pp. 127–168.

[10] N. N. Akhmediev, V. V. Afanasjev, and J. M. Soto-Crespo, Phys. Rev. E **53**, 1190 (1996); N. N. Akhmediev and V. V. Afanasjev, Phys. Rev. Lett. **75**, 2320 (1995).

[11] C. Pare, L. Gangnon, and P-A. Belanger, Opt. Commun. **74**, 228 (1989).

[12] G. Khitrova, H. M. Gibbs, Y. Kawamura, H. Iwamura, T. Ikegami, J. E. Sipe, and L. Ming, Phys. Rev. Lett. **70**, 920 (1993).

[13] V. G. Kulushkin, Sov. J. Quantum Electron. **17**, 116 (1987).

[14] M. Vaupel, C. Seror, and R. Dykstra, Opt. Lett. **22**, 1470 (1997).

[15] M. Vaupel, O. Mandel, and N. R. Heckenberg, J. Opt. B: Quantum Semiclassical Opt. **1**, 96 (1999).

[16] O. Cohen, T. Carmon, M. Segev, and S. Odoulov, Opt. Lett. **27**, 2031 (2002).

[17] A. A. Zozulya and D. Z. Anderson, Phys. Rev. A **51**, 1520 (1995).

[18] A. V. Mamaev, M. Saffman, and A. A. Zozulya, Phys. Rev. Lett. **76**, 2262 (1996).

[19] A. V. Mamaev, M. Saffman, D. Z. Anderson, and A. A. Zozulya, Phys. Rev. A **54**, 870 (1996).

[20] D. Z. Anderson, A. A. Zozulya, A. V. Mamaev, and M. Saffman, Phys. Rev. A **57**, 522 (1998).

[21] P. Yeh, IEEE J. Quantum Electron. **25**, 484 (1989).

[22] I. Oda, Y. Otani, L. Liu, and T. Yoshizawa, Opt. Commun. **148**, 95 (1998).

[23] N. Bekki and K. Nozaki, J. Phys. Soc. Jpn. **53**, 1581 (1984).

[24] N. N. Akhmediev, V. V. Afanasjev, and J. M. Soto-Crespo, J. Opt. Soc. Am. B **13**, 1439 (1996).

[25] B. I. Sturman and V. M. Fridkin, *The Photovoltaic and Photorefractive Effect in Noncentrosymmetric Materials* (Gordon and Breach, Philadelphia, 1992).

[26] In some conditions, additional background irradiance can allow a transition between focusing and defocusing nonlinearities in some PV-PR crystals, such as $LiNbO_3$, seeing C. Anastassiou, M. F. Shih, M. Mitchell, Z. G. Chen, and M. Segev, Opt. Lett. **23**, 924 (1998).

[27] Z. G. Chen, M. Segev, T. H. Coskun, and D. N. Christodoulides, Opt. Lett. **21**, 1436 (1996).

[28] Z. G. Chen, M. Segev, T. H. Coskun, D. N. Christodoulides, and Y. S. Kivshar, J. Opt. Soc. Am. B **14**, 3066 (1997).